Acta Biomaterialia 140 (2022) 314–323

Contents lists available at ScienceDirect

Acta Biomaterialia

journal homepage: www.elsevier.com/locate/actbio

Full length article

Bidirectional cell-matrix interaction dictates neuronal network formation in a brain-mimetic 3D scaffold

Sumanta Samanta[a], Laura Ylä-Outinen[b,c], Vignesh Kumar Rangasami[a], Susanna Narkilahti[b], Oommen P. Oommen[a,*]

[a] Bioengineering and Nanomedicine Group, Faculty of Medicine and Health Technology, Tampere University, 33720 Tampere, Finland
[b] NeuroGroup, Faculty of Medicine and Health Technology, Tampere University, Tampere, Finland
[c] Faculty of Sports and Health Sciences, University of Jyväskylä, Jyväskylä, Finland

ARTICLE INFO

Article history:
Received 27 July 2021
Revised 4 December 2021
Accepted 7 December 2021
Available online 10 December 2021

Keywords:
Neuronal network
Human pluripotent stem cells
Hyaluronic acid
Chondroitin sulfate
Dopamine
Brain-mimetic hydrogel scaffold

ABSTRACT

Human pluripotent stem cells (hPSC) derived neurons are emerging as a powerful tool for studying neurobiology, disease pathology, and modeling. Due to the lack of platforms available for housing and growing hPSC-derived neurons, a pressing need exists to tailor a brain-mimetic 3D scaffold that recapitulates tissue composition and favourably regulates neuronal network formation. Despite the progress in engineering biomimetic scaffolds, an ideal brain-mimetic scaffold is still elusive. We bioengineered a physiologically relevant 3D scaffold by integrating brain-like extracellular matrix (ECM) components and chemical cues. Culturing hPSCs-neurons in hyaluronic acid (HA) gels and HA-chondroitin sulfate (HA-CS) composite gels showed that the CS component prevails as the predominant factor for the growth of neuronal cells, albeit to modest efficacy. Covalent grafting of dopamine (DA) moieties to the HA-CS gel (HADA-CS) enhanced the scaffold stability and stimulated the gel's remodeling properties by entrapping cell-secreted laminin, and binding brain-derived neurotrophic factor (BDNF). Neurons cultured in the scaffold expressed Col1, Col11, and ITGB4; important for cell adhesion and cell-ECM signaling. Thus, the HA-CS scaffold with integrated chemical cues (DA) supported neuronal growth and network formation. This scaffold offers a valuable tool for tissue engineering and disease modeling and helps in bridging the gap between animal models and human diseases by providing biomimetic neurophysiology.

Statement of significance

Developing a brain mimetic 3D scaffold that supports neuronal growth could potentially be useful to study neurobiology, disease pathology, and disease modeling. However, culturing human induced pluripotent stem cells (hiPSC) and human embryonic stem cells (ESCs) derived neurons in a 3D matrix is extremely challenging as neurons are very sensitive cells and require tailored composition, viscoelasticity, and chemical cues. This article identified the key chemical cues necessary for designing neuronal matrix that trap the cell-produced ECM and neurotrophic factors and remodel the matrix and supports neurite outgrowth. The tailored injectable scaffold possesses self-healing/shear-thinning property which is useful to design injectable gels for regenerative medicine and disease modeling that provides biomimetic neurophysiology.

1. Introduction

The brain is a complex organ controlling numerous physiological processes and functions regulated by interconnected neuronal networks. These neuronal networks form the key communication channels and are vital for all physiological activities. However, traumatic brain injury (TBI) and brain hemorrhage cause damages to this neuronal network leading to morbidity and mortality in humans [1,2]. Although neurons in the adult human brain are known to possess poor regenerative capabilities, the tissue engineering (TE) strategies that utilize stem cells and extracellular matrix (ECM) mimetic scaffolds offer promising solutions to regenerate damaged neural tissue of the central nervous system (CNS) [3].

* Corresponding author.
E-mail address: oommen.oommen@tuni.fi (O.P. Oommen).

https://doi.org/10.1016/j.actbio.2021.12.010

However, there is a need to develop an injectable 3D scaffold that provides an ideal niche for transplantable neuronal cells promoting neural maturation, neurite outgrowth, and overall support for the regeneration of the soft brain tissue [4]. Such scaffolds which emulate the native brain tissue also allow us to study the intricate cellular networks of the brain and cell-matrix interactions in vitro. Thus, these brain mimetic 3D scaffolds could be exploited as in vitro brain models which have an enormous potential for CNS disease modeling [5,6], drug discovery [7], and toxicological studies [8].

Several attempts have been made to design TE-based brain models using Matrigel [9], silk fibroin [10,11], alginate gels [12–14], chitosan gels [15], polyethylene glycol PEG-derived [16], and 3D-printed rigid [17,18] scaffolds using two-photon polymerization for longer culture. However, to design a brain extracellular matrix (ECM) mimetic 3D scaffold for clinical applications, it is imperative to understand the ECM composition and mechanics of the brain tissue. Roughly, 10–20% of the total brain ECM is composed of glycosaminoglycans such as chondroitin sulfate (CS), hyaluronic acid (HA), and lecticans such as aggrecan, phosphacan, versican, and neurocan [19]. Since HA and CS are the major components of the brain ECM, several research groups have designed scaffolds based on HA [20] and CS [21] for culturing neuronal cells of various origins. Most of the 3D scaffold studies reported in literature utilize rodent-derived neuronal cells and organotypic brain slice cultures. However, studies utilizing primary human or pluripotent stem cell (hPSC) derived neurons [18,22,23] are limited due to challenges in culturing human pluripotent cells. Though the rodent-based neuronal cultures and organotypic brain slice cultures have advanced our understanding of the brain network and function, the human and rodent neuronal cells act significantly different [24] and rodent neuronal cells do not recapitulate human neurophysiology [25]. Thus, developing 3D scaffolds that support the growth of hPSC-derived human neuronal cells and provide biomimetic neurophysiology is useful to develop disease models and study the complexity of neuroscience.

Neuronal and glial cells in the brain tissue interact with the ECM bi-directionally regulating cell state, fate, maturation, differentiation, and survival. Moreover, these cells also remodel the ECM by secreting biochemical factors and other proteins [26]. Matrix metalloprotease 10 (MMP-10) is one of such enzymes that play a vital role for neuronal cells, as these enzymes degrade ECM proteins such as collagen IV, laminin, and fibronectin [27] and regulate neuronal network formation. We have earlier shown that MMP-10 participates in the regulation of attachment and migration of hPSC-derived neuronal cells [28]. Other ECM proteins such as collagens and laminins are also expressed by human neuronal cells under promotive culture conditions and play important roles as adhesion molecules for neuronal cell adhesion, survival, and outgrowth [28,29] that the protein, integrin $\alpha 6\beta 4$ is a key neuronal cell-specific integrin for laminins and thus plays an important role in neuronal cell-ECM interaction signaling [22]. Thus, the expression of these proteins by the hPSC-derived human neuronal cells could be used as a benchmark for the comparison of favorable neuronal maturation as a result of 3D culture.

In this article, we aim to identify a 3D scaffold that promotes neuronal network formation and study the bi-directional scaffold-neuronal cell interactions using human induced pluripotent stem cells (hiPSC) and human embryonic stem cells (hESC) derived neuronal cells.

2. Materials and methods

Hyaluronic acid (MW 130 kDa) was purchased from LifeCore Biomedical (Chaska, USA). Dopamine (2-(3,4-Dihydroxyphenyl) ethylamine hydrochloride), 1-ethyl-3-(3-dimethylamino propyl)-carbodiimide hydrochloride (EDC), 1-hydroxy benzotriazole hydrate (HOBt), N-hydroxysuccinimide (NHS), Carbohydrazide (CDH), 3-amino 1,2- propanediol, Sodium periodate and Chondroitin sulfate A sodium salt from bovine trachea were purchased from Sigma-Aldrich. The short laminin peptide with 12 AA sequence (CCRRIK-VAVWLC) was obtained from GenScript, USA. Dialysis membranes used for purification were purchased from Spectra Por-6 (MWCO 3500). All solvents were of analytical quality. All spectrophotometric analysis was carried out on Shimadzu UV-3600 plus UV–vis–NIR spectrophotometer. The NMR experiments (δ scale) were recorded with JEOL ECZR 500 instruments, operating at 500 MHz for ^{1}H.

2.1. Preparation of hydrogels

The hydrogels were prepared using conventional hydrazone cross-linking chemistry. Briefly, hydrazide modified HA (HA-CDH or HADA-CDH) were dissolved in 10% sucrose solution, and aldehyde modified polymer (HA-Ald, CS-Ald, or CS-Ald(lam)) are separately dissolved in PBS (pH 7.4) to reach a concentration of 14 mg/mL. Synthesis of the components is described in detail in supporting information (SI 1.1- SI 1.5). The transparent gels were prepared by mixing the equal volumes of aldehyde and hydrazide derivatives of polymers to obtain the following groups: HA-HA gel, HA-CS gel, HADA-HA gel, HADA-CS gel, HA-CS(lam), and HADA-CS(lam) gels.

2.2. Rheological studies of hydrogels

We estimated the viscoelastic properties of HA-HA, HA-CS, HADA-HA, and HADA-CS hydrogels using TA instruments DHR-II instrument by measuring the gel deformation with a frequency sweep method which enabled the measurement of storage and loss modulus as a function of frequency. The linear viscoelastic region (LVR) of each of the 250 µL gels (diameter = 12 mm, height = 1.5 mm) were determined first by an amplitude sweep at a constant frequency of 1 Hz to find out the strain rate, which was determined to be 1% that we used as a constant to run the frequency sweep between 0.01 to 10 Hz. Average mesh size (ξ) and Average molecular weight between crosslinks (M_c) were also determined following rubber-elastic theory [30]. All rheological characterizations of the hydrogels were performed in the absence of cells (N = 3).

2.3. Hydrogel degradation and stability studies

To study the stability and swelling behavior of the hydrogels, three parallel samples (N = 3) of hydrogels (HA-HA, HADA-HA, HA-CS, and HADA-CS) were immersed in a neuronal cell culture medium. Briefly, 250 µL gels were prepared in glass vials and the initial weight of the hydrogels was obtained. The gels were then submerged in one mL of cell culture medium. To observe the swelling and subsequent degradation characteristics of the gels, the gels were weighed, and the medium was replaced daily for the first four days. Subsequently, after the first four days, the media was replaced every alternate day for two weeks. The remaining weight percentage was calculated by using the following formula:

$$\text{Remaining weight\%} = \frac{(\text{Measured weight})}{(\text{Initial Weight})} \times 100$$

We have also checked the stability of these hydrogels submerged in the medium by measuring the storage modulus using a rheometer as mentioned in the earlier section. The medium was removed, the hydrogels were transferred to the bottom plate of the rheometer, and measurements were performed. We chose three different time points, day 1, day 7, and day 14. The storage modulus of the gels at these time points was compared to each hydrogel

prior to the addition of any medium and the experiment was conducted in triplicate (N = 3).

2.4. Cells and cell culture

Two cell lines were used in this study; Regea08/023 (hESCs) and UTA04511.WTs (hiPSCs). Stem cells were maintained and differentiated into cortical neuronal cells with the previously described method [31]. Shortly, stem cells were first plated onto laminin (LN521, Biolamina) coated surface in presence of 100 nM LDN193189 and 10 µM SB431542 (both from Sigma) for neural induction. Thereafter, in the neural proliferation stage, 20 ng/mL fibroblast growth factor-2 (FGF2, Thermo Fisher Scientific) was used as a supplement. Finally, cells were detached with StemPro Accutase (Thermo Fisher Scientific) and plated inside the gels in this neuronal maturation stage and the medium was supplemented with 20 ng/mL brain-derived neurotrophic factor (BDNF, R&D Systems), 10 ng/mL glial-derived neurotrophic factor (GDNF, R&D Systems), 500 µM dibutyryl-cyclicAMP (db-cAMP, Sigma) and 200 µM ascorbic acid (AA, Sigma). The hPSCs used in this study were acquired from voluntary subjects who had given written and informed consent. The institute has a supportive statement from Pirkanmaa Hospital District to generate IPSCs from donor cells (R08070) and to use generated cell lines in neuronal research (R05116).

2.5. Immunostaining

Immunostaining was performed by following the protocol that has been published previously [22,32]. Shortly, cells were fixed in 4% paraformaldehyde, followed by a blocking step using 10% normal donkey serum (NDS), 0.1% Triton-X 100, and 1% bovine serum albumin (BSA) (all from Sigma-Aldrich) for 1 h at room temperature. Then, primary antibodies, β-tubulin III (mouse; 1:1500; T8660, Sigma-Aldrich), microtubule-associated protein 2 (MAP2; chicken; 1:4000; NB300-213, Novus Biologicals, Littleton, CO, USA), synaptophysin (rabbit, 1:1000, ab32127, Abcam), and laminin (mouse, 1:400, ab115575, Abcam) were incubated 48 h followed by intensive washing. Secondary antibodies conjugated with Alexa 488, 568, or 647 (A21206, A21043, A21449, respectively, Thermo Fisher Scientific) were used at a 1:400 dilution, with 12 h incubation followed by final washes including the addition of 4',6-diamidino-2-phenylindole (DAPI).

2.6. qPCR study

The hiPSCs and hESCs derived neuronal cells were cultured in our test hydrogels (N = 5 for each group) and the RNA was extracted on day 1 and day 14. The fold changes in gene expression on day 14 (relative to day 1) were obtained for hiPSCs and hESCs separately and were averaged and presented in Fig. 4. For the gene expression analysis hydrogels were lysed by mechanical disruption and the encapsulated cells were collected using a cell strainer before obtaining total RNA with an RNEasy Plus mini kit (Qiagen). 60 ng of the total RNA was used to prepare cDNA. For cDNA synthesis, a commercial high-capacity cDNA reverse transcription kit (Applied Biosystems) was used according to the manufacturer's protocol. The qPCR was performed using BioRAd CFX1000. The PCR primers used (TaqMan Gene Expression Assay, Thermo Fisher Scientific) were GAPDH (Assay ID: Hs02786624_g1), COL11 (Hs01097629_g1), MMP10 (Hs00233987_m1), COL1 (Hs00164004_m1), TUBB3 (Hs00801390_s1), and ITGB4 (Hs00236216_m1).

2.7. Data analysis and statistics

All image information obtained at least two repetitive experiments. Detailed information about imagining and image preprocessing is found from Supplementary material (Supplementary material 1.9) 3D rendering and numerical measurements from 3D reconstructions performed using Imaris (Bitplane AG, Zürich, Switzerland) volumetric rendering followed by neuronal tracking using the same parameters for each image to ensure comparability. Statistical significance was evaluated using the Kruskall-Wallis t-test followed by Dunn's Multiple Comparison test (GraphPad Prism, GraphPad Software, San Diego, CA, USA) for the immunostained images to analyze neurite number (N = 5 per group), neurite length (N = 5 per group), and laminin expression (N = 7 per group). Differences were considered to be significant with P-value < 0.05. qPCR data were normalized and analyzed using a comparative quantitation method and data are presented as $\Delta\Delta$Ct method and normalized against cells cultured in respective hydrogel conditions at day one. The reference housekeeping gene GAPDH was selected as an internal control for the normalization of qPCR data. The efficiency of endogenous control amplification was approximately equal to the amplification of target genes. Statistical significances were evaluated using the Mann-Whitney test (GraphPad Prism, GraphPad Software, San Diego, CA, USA).

3. Results and discussion

To design an ideal ECM mimetic matrix that could efficiently stimulate the hiPSC and hESC-derived human neuronal cells to grow and form networks, we decided to use HA and CS as building blocks as they constitute the major ECM component of the native brain tissue. Although HA is commonly used for designing 3D matrices, the CS polymer is not often added. CS and its' proteoglycan (CSPG) derivatives, such as aggrecan are frequently found in the brain tissue and play a crucial role in the brain development, anchoring, and expansion of the perineural net in the cortex [33]. CS is also known to tether neurotropic agents and possess binding sites to integrins [34]. These properties of CS are suggested to support neuronal growth and maturation [33]. Thus, CS-based matrices are used to encapsulate FGF-2 which led to the promotion of neuroprotection and rat primary neural stem cell maintenance in post-TBI [35]. Here, we designed HA gels and HA-CS composite gels using a hydrazone-based dynamic covalent crosslinking strategy exploiting carbodihydrazide (CDH) and aldehyde-modified components. We have earlier demonstrated that the hydrazone crosslinks formed between the CDH and aldehyde functionalized HA display exceptionally stable covalent linkages [36] and thus can be used for 3D matrix forming and tissue engineering applications [37]. The degree of crosslinking was tuned to be 10–12% to obtain gels with comparable viscoelastic properties. We also covalently grafted dopamine (DA) to our 3D scaffolds as we have earlier shown that DA-containing scaffold provides tissue adhesive properties and improves the stability of the hydrogel in the medium [38]. We anticipated that incorporation of DA for designing a 3D matrix for hPSC derived neuronal culture would offer several advantages, such as (a) it could enhance the stability of the matrix in cell culture medium, (b) DA possessing a tissue adhesive property could bind and trap cell-secreted ECM proteins and remodel the matrix, and (c) DA being a neurotransmitter that plays a key role in axon growth and synapse formation during embryogenesis, it could be advantageous for maturation of neurons [39].

Thereafter, we systematically characterized the viscoelastic behavior of HA-HA gel and HA-CS and the DA functionalized gels (namely, HADA-HA and HADA-CS) (Fig. 1) following the frequency sweep (Fig. 2A). We obtained impressive storage modulus for all the gels at 1 Hz frequency (853±51, 748±63, 789±22, and 960±55 Pa for HA-CS, HADA-CS, HA-HA, and HADA-HA respectively). All the gels showed consistently higher storage modulus than loss modulus within the frequency range of 0 to 10 Hz demonstrating the viscoelastic nature of the gels. On the other hand, the ratio be-

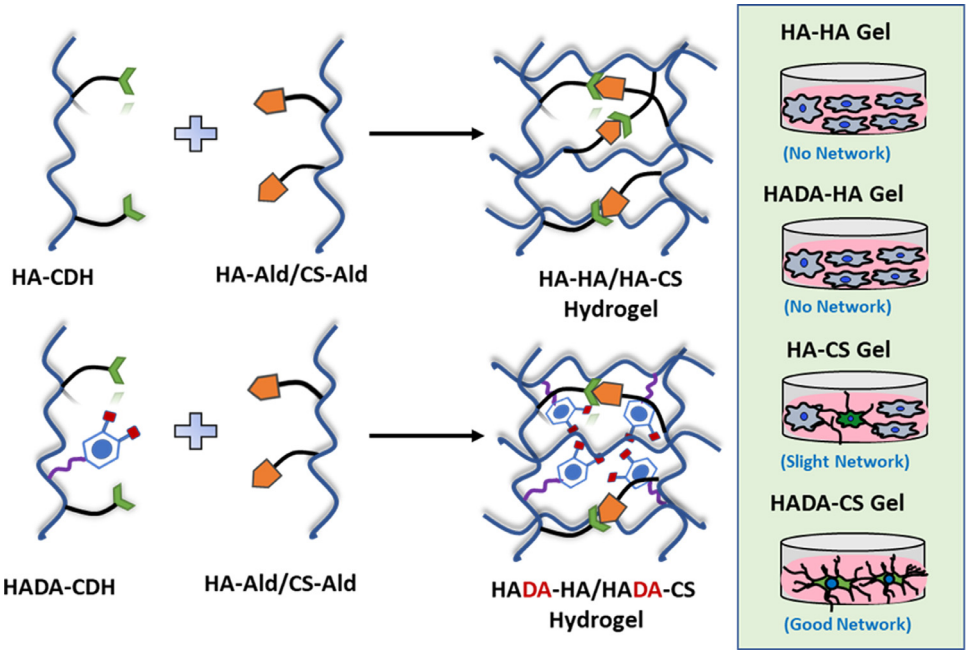

Fig. 1. Schematic representation of hydrogel preparation and neuronal network formation.

tween loss and storage modulus, represented by tan δ, displayed a significantly lower value than 1 (ranging between 0.0043 to 0.0078) for all the four gels, implying a highly elastic nature of the four gels. We also determined the pore size (ξ) of the gels using the rubber elastic theory from the storage modulus values. While the conjugation of DA in the HA-HA gels (HADA-HA gel) resulted in a stiffer matrix yielding a smaller pore size of the scaffolds (16.24 nm) compared to the HA-HA scaffold (17.34 nm), the same phenomenon was not observed in the case of HA-CS gels (16.90 nm) compared to HADA-CS gels (17.65 nm). However, calculations of average molecular weight between the crosslinks (M_c) suggest the similar matrix nature of HA-HA (34.07 kg/mol) and HA-CS gels (33.97 kg/mol). The smaller Mc in the case of HADA-HA gels (27.94 kg/mol) compared to the HADA-CS gels (39.21 kg/mol) indicated the more compact matrix nature in the case of the former. In general, incorporation of covalently grafted DA in either HA-HA and HA-CS gels significantly altered the storage modulus, average pore size, and average molecular weight between the crosslinks (Table S1).

Next, we estimated the swelling and degradation of all these four gels under physiological conditions without cells (PBS, pH 7.4 and neuronal cell culture medium) for two weeks (Fig. 2C). We chose the two conditions as the viscoelasticity and stability of the hydrogel can be modulated by the soluble proteins present in the cell culture matrix (in cell free hydrogels) or by the metalloproteases and other ECM proteins secreted by the encapsulated cells (in cell laden hydrogels). Fascinatingly, none of the gels exhibited a high degree of swelling within this period, however, the storage modulus changed significantly for the gels, when they were immersed in culture medium on day 14 (Fig. 2D). Compared to the gels without medium, we observed substantial loss of mechanical integrity of the matrix in case of HA-HA and HA-CS gels, as the storage modulus sharply dropped from 789 Pa to 191.5 Pa and 853 Pa to 485 Pa, respectively, after day 1. Fascinatingly, the presence of DA in the scaffold significantly enhanced the matrix stability in the medium, as evidenced from the 960 Pa to 895 Pa in the case of HADA-HA and 748 Pa to 714 Pa in the case of HADA-CS gels. Except for HA-HA gels, the matrix modulus did not change drastically for all the other three gels until day 7, albeit after day 14, the modulus dropped substantially. It is interesting to note that although we did not observe a significant change in the hydrogel swelling on day 14 for any of the gels, the modulus values decreased for all of them. Although the physical weight of the gels did not change considerably, the cross-linking density was reduced significantly resulting in softer yet robust gels. We believe entanglement-driven cross-linking besides chemical crosslinking plays a key role in stabilizing the bulk hydrogel structure [40]. The softer gels presumably will play a key role in advancing neuronal network formation. To determine the injectability of these cross-linked hydrogels, we first measured the flow behavior (viscosity) at room temperature (Fig. 2B) by continuously increasing the shear rate. All these hydrogels displayed a rapid decline in the viscosity upon application of increasing shear rate (0.01 to 2 s^{-1}) suggesting that all these four hydrogels are injectable. We further determined the shear-thinning/self-healing characteristics of these gels by estimating the viscosity recovery (i.e., the ability of the gels to undergo gel-to-sol transition under high strain conditions which recover back to original gel state without loss in viscosity under low strain conditions) by performing a dynamic shear-thinning experiment. This was performed by applying a periodic low (0.01 s^{-1}) and high shear rate (10 s^{-1}) to the test hydrogel samples (seven cycles; Fig. 2E and Figure S4 in SI). All the hydrogels recovered their initial viscosity when the shear rate was periodically lowered. We also tested the dynamic strain recovery properties of these hydrogels. (Fig. 2F and Fig. S5 in SI). At low strain (1%), all the hydrogels show higher storage modulus, and with increasing strain (50%) the storage modulus reduces while loss modulus increases. Except with HADA-CS hydrogel, storage modulus is always higher than loss modulus. Upon withdrawal of the high strain, all the hydrogels recover their initial storage modulus suggesting the dynamic nature of the crosslinking chemistry. Such viscoelastic characteristics of the ECM mimetic gels are particularly advantageous for designing injectable scaffolds for tissue regenerative applications, especially for stem cell delivery.

After analyzing the rheological properties of the hydrogels, we conducted in vitro studies to analyze if our hydrogels support the growth of hPSC-derived neuronal cells. As laminin-mimetic peptide IKVAV is known to promote neuronal cell adhesion to matri-

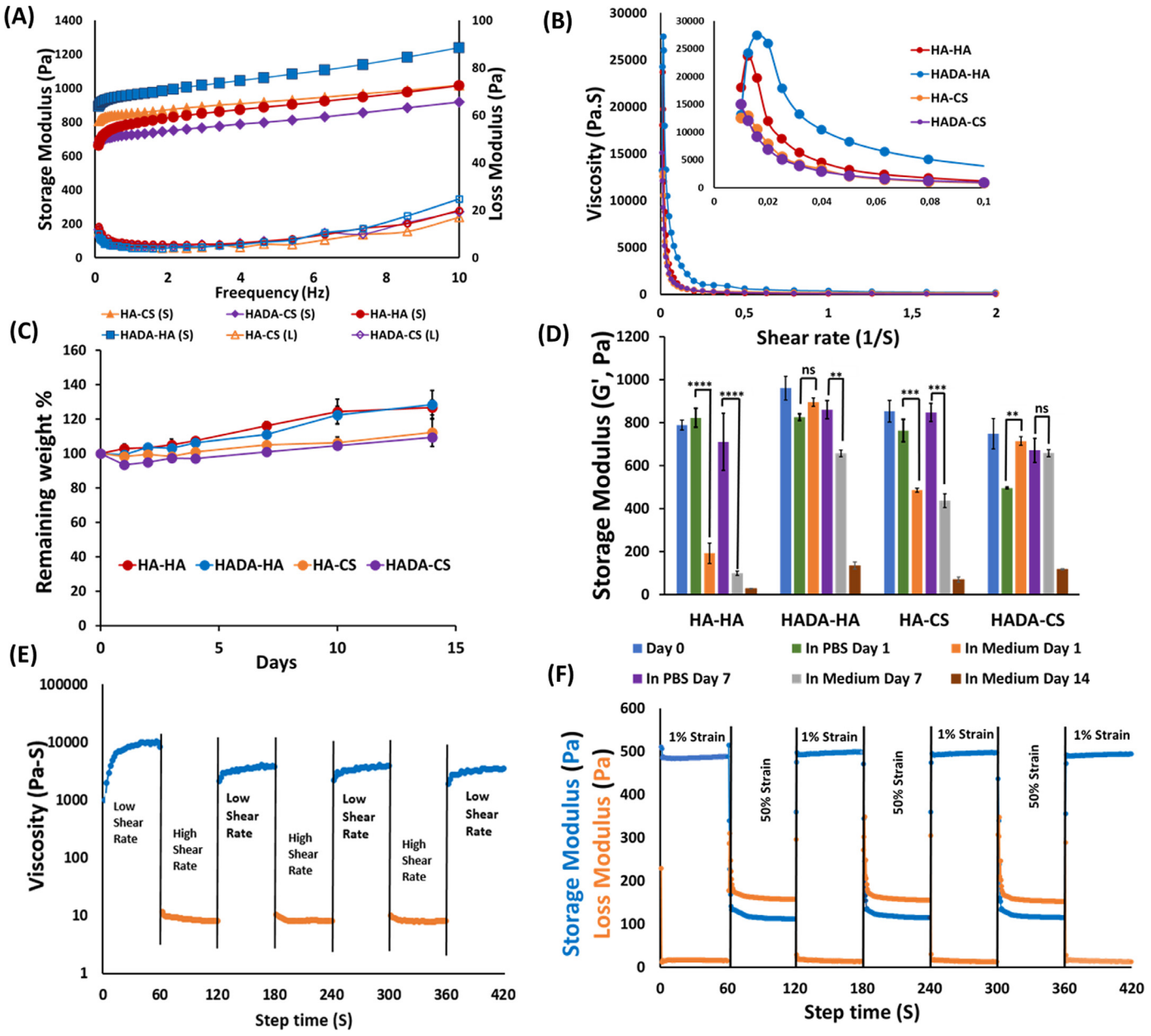

Fig. 2. Viscoelastic properties and degradation behaviors in gel compositions. (A) Rheological analyses of HA-HA, HA-CS, HADA-HA, and HADA-CS hydrogels ('S' and 'L' in the parenthesis at the legend denotes storage and loss modulus respectively) (N = 3). (B) Flow property of these gels within a continuous increasing shear rate of 0.01 S^{-1} to 2 S^{-1}. (C) Swelling behavior of these gels in the neuronal medium until two weeks (N = 3), and (D) Change in storage modulus (G′, Pa) of these gels in presence of medium and PBS at different time points, day 1, day 7, and day 14 (statistics: Two-way ANOVA Turkey HSD for multiple comparisons) (N = 3), (E) Shear-thinning/self-healing property of HADA-CS hydrogel immersed in PBS at day 1 undergoing cyclic deformation of low shear rate (0.01 s^{-1}) and high shear rate (10 s^{-1}), and (F) Dynamic strain recovery of a HADA-CS hydrogel undergoing cyclic deformation of 1% (low) and 50% (high) strain at 1 Hz with G′ (blue line) and G″ (orange line). (For interpretation of the references to color in this figure legend, the reader is referred to the web version of this article.)

ces lacking integrin-binding sites (such as HA gels) [41], we conjugated the cysteine terminated IKVAV peptide by thiazolidine linkage following the condensation reaction between the N-terminal cysteine and aldehyde moiety [42]. We encapsulated the hiPSC and hESC-derived neuronal cells in our hydrogels namely, HA-HA, HA-CS, HADA-HA, and HADA-CS gels as well as gels conjugated with laminin mimetic peptide conjugated matrices namely, HA-HA(lam) and HA-CS(lam). After 14 days of culture in the 3D matrix, we performed immunocytochemical staining to quantify the expression of key neuronal markers, β-tubulin$_{III}$ and MAP-2 to ascertain the maturation of neuronal cells and formation of neuronal networks. Staining failed to illuminate any neurite outgrowth of hiPSC-derived neuronal cells in HA-HA gels (Fig. 3A). This suggests that HA gels do not support the maturation of hiPSC-derived neuronal cells. Next, we evaluated the HA-CS composite gels. Fascinatingly, the HA-CS gels displayed neurite outgrowth as evidenced by the increase in the MAP-2 and β-tubulin$_{III}$ expression (Fig. 3B). This suggests that the cells perceive the sulfated matrix composition stimulating neuronal cell maturation. To our surprise, incorporation of IKVAV peptide to the HA-CS matrix (HA-CS(lam)) blocked this beneficial effect and disturbed the neurite outgrowth as demonstrated by the absence of the neuronal markers in these scaffolds (Fig. 3C). We hypothesize that the incorporation of cationic IKVAV peptide masked the anionic sulfate groups of the CS backbone and abolished the beneficial effect of CS.

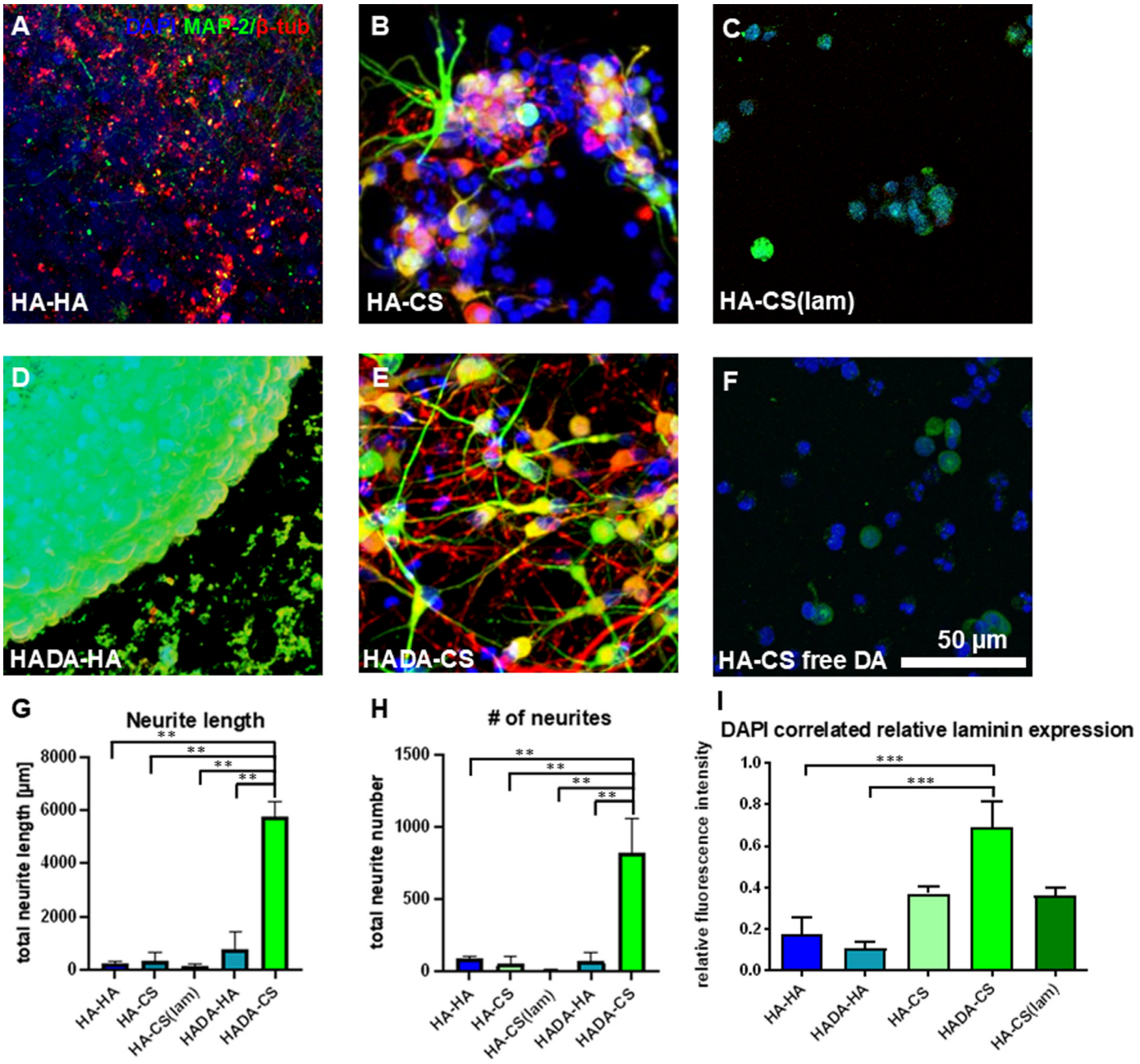

Fig. 3. Neurite outgrowth, network formation, and laminin expression in different gel compositions. hiPSC derived neuronal cells encapsulated within (A) HA-HA (non-viable culture), (B) HA-CS (healthy culture with weak neurite outgrowth), (C) HA-CS(lam) (neurites absent), (D) HADA-HA (strong aggregation), (E) HADA-CS (healthy culture with abundant dendritic presence), (F) HA-CS free DA (neurites absent) hydrogels for 14 days and immunostained against MAP-2 (green, common neuronal marker, staining dendrites) and β-tubulinIII (β-tub, red, a common neuronal marker, staining axons). DAPI (staining cell nuclei) is shown as blue. All images are maximum intensity projections of confocal stacks. (Scalebar = 50 µm) (G) Total neurite length of each neuronal network measured from the 3D render of the confocal stack (N = 5 for each group). (H) The number of neurites (N = 5) of each neuronal network measured from the 3D render of the confocal stack. Five blocks, 150 µm × 150 µm × 150 µm, are analyzed from each gel composition. (I) hESC-derived neuronal cells grown in HA-HA, HADA-HA, HA-CS(lam), HADA-CS, and HA-CS gel were analyzed for laminin protein secretion by correlating laminin fluorescence to DAPI expression in each region of interest (ROI, N = 7 ROIs/sample). Data are expressed as relative laminin staining fluorescence intensity normalized against DAPI intensity. Statistical significance: $^{*}= p< 0.05$, $^{**}= p<0.01$ $^{***}=p<0.001$. (For interpretation of the references to color in this figure legend, the reader is referred to the web version of this article.)

As coating of cell culture plate with polymer functionalized with DA [43] or DA functionalized into a bioink are reported to enhance neuronal regeneration [44], we investigated the DA functionalized hydrogels. The DA conjugated HA-HA hydrogels (HADA-HA) did not show any neuronal maturation of hiPSC-derived neuronal cells and instead promoted the aggregation of the cells as seen in Fig. 3D. On the contrary, the HA-CS gels functionalized with DA (HADA-CS) displayed astonishing neurite outgrowths (Fig. 3E). Such exceptional neuronal network formation is not reported with hiPSC-derived neuronal cells in any glycosaminoglycan-derived hydrogels. In order to decipher the role of DA in stimulating this effect, we doped the HA-CS gels with 150 nmoles of free DA molecules and cultured the hiPSC-derived neuronal cells. Under these conditions, we found that the maturation of hiPSC-derived neuronal cells was completely abolished as no neurite outgrowth was observed (Fig. 3F). This equivocally demonstrates that the DA molecules do not directly stimulate the hiPSC-derived neuronal cells to undergo maturation, instead, the covalent conjugation of

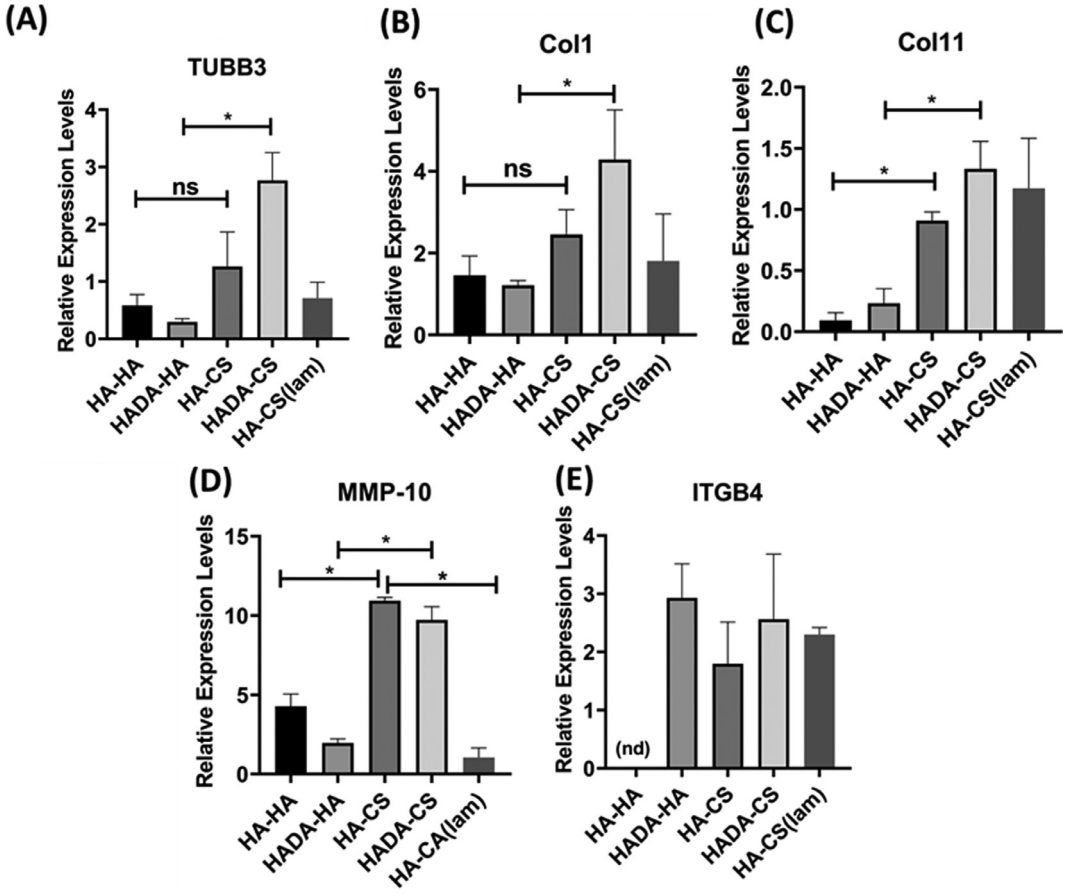

Fig. 4. Average of the gene expression of hiPSCs and hESCs derived neuronal cells cultured inside the hydrogels at day 14 compared to day 1. (A) TUBB3, (B) Col1, (C) Col11, (D) MMP10, and (E) ITGB4 expressions at day 14 normalized to day 1 expressions of each gel composition. Statistical significance: $^{*}= p< 0.01$ (nd: not detected) (N = 5).

DA on the scaffold indirectly supports the cell growth. We substantiated the matrix property on neuronal cell maturation using both hiPSCs and hESCs-derived neurons (Figure S7 in SI)

To further quantify the ability of the hydrogels to support the growth of the hiPSC-derived neuronal cells, we measured the number of neurites formed and their length numerically from images obtained after the immunostaining using Imaris software (Bitplane AG, Switzerland). Numerical data suggests that HADA-CS hydrogels promote an extensive neuronal network formation compared to HA-CS and HADA-HA gels. The total neurite length supported by the HADA-CS, HA-CS, and HADA-HA was 41.6×10^3 µm vs. 1.1×10^3 µm and 1.1×10^3 µm, respectively (Fig. 3G). Accordingly, the number of detected neurites was clearly the highest in the HADA-CS group (Fig. 3H) when compared to all the other groups thereby suggesting that functionalizing the DA to HA-CS hydrogel stimulated the hiPSC-derived neuronal cells and promoted enhanced neuronal outgrowth and network formation. Thus, our study clearly shows that both CS and DA are key components in designing 3D matrices for good neuronal outgrowth. Moreover, the DA molecule needs to be covalently linked to the gel backbone since free DA addition did not support neuronal cell growth in HA-CS gels.

We hypothesize that the substrate-bound DA molecules and sulfated GAGs provide the haptotactic cues by entrapping the cell-produced ECM molecules to remodel the 3D matrix and regulate the cellular-matrix interactions. In order to verify the growth factor binding capability to assist matrix remodeling by HADA-HA and HADA-CS hydrogels, we performed a release experiment of encapsulated brain-derived neurotropic factor (BDNF) from these gels and quantified the release of active protein by ELISA. Interestingly, we observed only ~24% BDNF release from the HADA-CS gels, whereas ~74% of BDNF was released from HADA-HA gels after 7 days (Fig. S6 in SI). To further validate our results, we cultured hESC-derived neuronal cells and performed an immunostaining experiment to quantify the cell-secreted laminin (trapped within the gels) which plays a key role in neuronal cell maturation and network formation. Aligning with our hypothesis, the laminin secretion was significantly higher in HADA-CS gels compared to HA-HA and HADA-HA hydrogel compositions after 14 days of culture (Fig. 3I).

To further validate our findings on the bi-directional effect of matrix composition on hiPSC and hESC-derived neuronal cell response, we performed qRT-PCR analysis to estimate the expression of neuronal-specific genes. We cultured hiPSCs and hESCs derived neuronal cells in our hydrogels and performed a qRT-PCR experiment to quantify relative neuronal cell-specific gene expression in each group. The β-tubulin$_{III}$ encoded by the TUBB3 gene is a microtubule that is found in neuronal cells and acts as a key marker for neuronal cell maturation. We investigated the expression of TUBB3 in different hydrogel matrices on day 14 and compared that to the expression on day 1. Corroborating with the immunostaining data, the TUBB3 expression was significantly higher in HADA-CS gels and other CS-containing matrices when compared to the HADA-HA (Fig. 4A), demonstrating the significance of CS as part of brain mimetic hydrogel design that supports neuronal culture. We have earlier shown that the expression of the fibrous collagen gene serves as a promising marker for neuronal cell adhesion and spreading in the hydrogel matrix [28]. Thus, we esti-

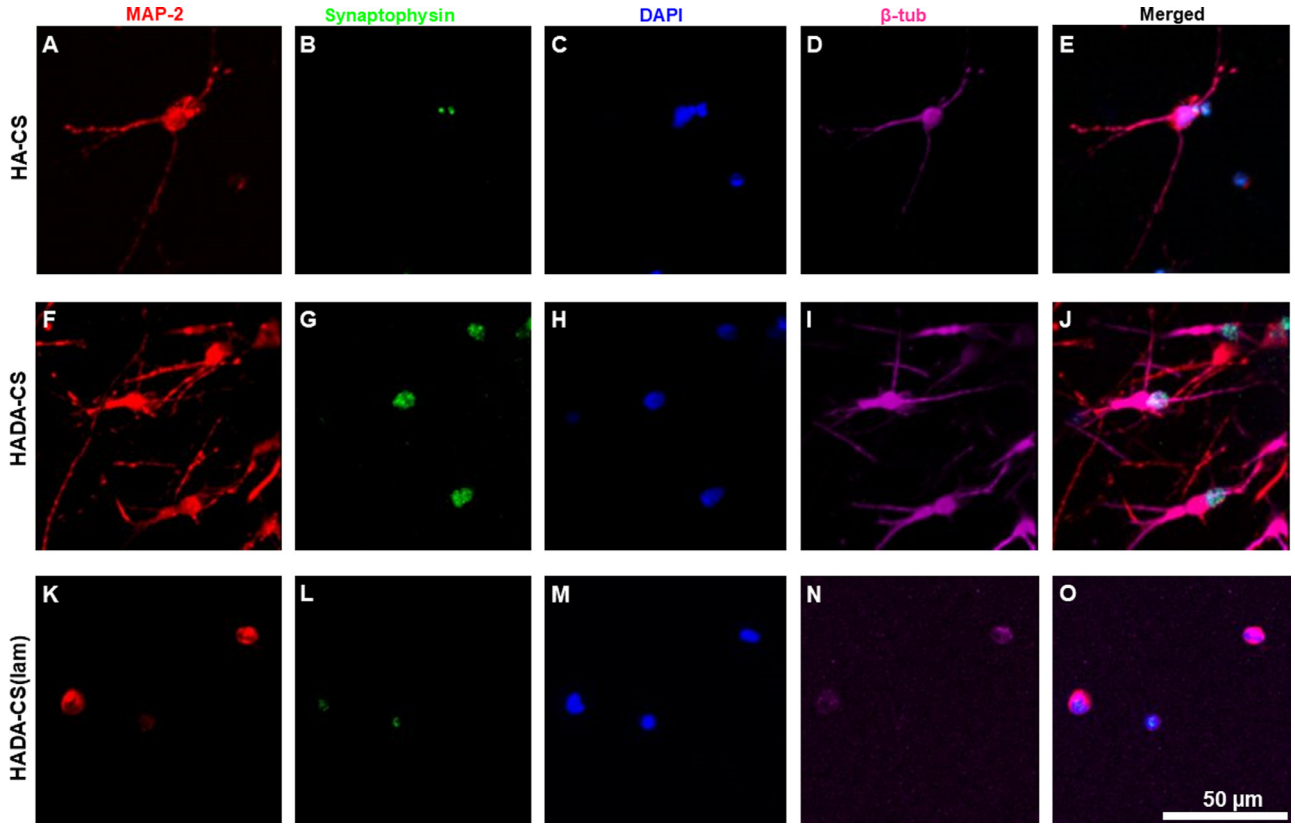

Fig. 5. Synaptophysin expression in the hiPSC derived neuronal cells grown in different gel compositions after 14 days of culturing inside the hydrogel. Cells grown in A-E) HA-CS, F-J) HADA-CS, and K-O) HADA-CS(lam) gel compositions were stained against MAP-2 (A,F,K), Synaptophysin (B,G,L), and b-tubulin (D,I,N) as well as with DAPI (C,H,M). Merged images with composed color representation for each gel: HA-CS, HADA-CS, and HADA-CS(lam) are shown in E, J, and O, respectively. Synaptophysin is localized to soma according to co-localization with DAPI. (Scalebar = 50 µm).

mated the expression of collagen-1 (Col1) and collagen-11 (Col11) gene expression in different gel compositions and found that the CS-containing gels displayed higher levels of these genes compared to non-CS-containing ones, with the highest expression in HADA-CS gels (Fig. 4B and 4C). This illustrates that CS plays an important part in the matrix composition for designing brain mimetic scaffold. Conjugation of DA further augments this effect. In order to stimulate neuronal network formation for establishing a neural circuit, the neuronal cells secrete metalloproteases (MMPs) which is a key regulator that induces structural plasticity [27]. MMP-10 is one such metalloprotease that is upregulated by the neurons in the human brain after ischemic injury [45]. Interestingly, we observed increased expression of MMP-10 after 14 days in matrices containing CS (Fig. 4D) that indicates the significance of CS in promoting matrix remodeling a key factor for stimulating neuronal network formation. Next, we quantified the expression of integrin-β 4 (ITGB4) which is an important marker for laminin-neuronal cell interactions [22]. ITGB4 expression can also be considered as a marker for hPSC-derived neuronal cell spreading and attachment [28]. Unlike other neuronal markers which displayed exclusive CS sensitivity, the ITGB4 was predominantly higher in DA-containing matrices suggesting that the tissue adhesive DA moiety and CS to some extent increase the integrin expression and promote neuronal spreading (Fig. 4E). Thus, in conjunction with the immunostaining data, the gene expression studies unequivocally demonstrate the significance of matrix composition and the neuronal cell-mediated matrix remodeling as the crucial factors for neuronal cell culture and network formation.

Finally, we showed the expression of synaptophysin in the neuronal cell culture to ascertain the maturation of the neurons. Synaptophysin is an essential protein that plays a part in synaptogenesis [31], and its expression in the cell soma shows that expression of synaptic components has been initiated in the neurons in 3D, yet not completed in synapse formation in axons [46,47]. According to staining, synaptophysin seems to be expressed more in HADA-CS encapsulated cells (Fig. 5G) compared to HA-CS (Fig. 5B) or HADA-CS(lam) (Fig. 5L) hydrogels at a 14-day time point. This result indicates that neuronal cells cultured in the HADA-CS matrix experiences a favorable 3D microenvironment, and support neuronal maturation and neurite outgrowth.

4. Conclusion

In conclusion, we have engineered brain-mimetic injectable hydrogel scaffolds with self-healing/shear-thinning properties. Our study demonstrates that composite gels comprising HA and CS have dynamic strain recovery properties and support neuronal cell culture. The CS in the hydrogel matrix mimics the role of chondroitin sulfate proteoglycan (CSPG) in the brain tissue and binds to neurotrophic factors produced by the neuronal cells and supports neuronal growth, self-renewal, and network formation. Incorporation of laminin mimetic peptide (IKVAV) to the brain mimetic matrix compromise this effect. Although HA-CS based composite matrix supports the hiPSC-derived neuronal cells, the chemical cues provided by the CS are not potent enough to support network formation. Covalent grafting of 4 mol% DA molecules (relative to the disaccharide units of HA) to the HA-CS gels supported matrix stability in neural medium and matrix remodeling as evidenced by high expression of laminin protein as observed in the immunostaining of the gels and increased gene expression of MMP-10 and integrin $\alpha 6\beta 4$ (ITGB4), which is a key laminin receptor expressed on neurons. Thus, the synergistic combination of chemical cues ex-

pressed by the CS and DA components in the HADA-CS matrix-supported cell-mediated ECM remodeling and stimulated the network formation of the hiPSC-derived neuronal cells. In the absence of sulfated GAGs, the HADA-HA gels did not show any advantage in neuronal differentiation despite the integrin $\alpha 6\beta 4$ expression and ECM proteins trapped in the gels, suggesting the combination of chemical cues and ECM remodeling is necessary for successful maturation of hiPSC-derived neurons. The dopamine grafted on the matrix enhances the haptotactic cues (e.g. collagen, and other tissue adhesive ECM molecules) and the CS component binds to chemotactic cues (e.g. neurotrophic factors) and this combination is vital for designing brain-mimetic scaffolds for neuronal regeneration. The role of dopamine was to promote ECM deposition and does not induce cell signaling that promotes neuronal differentiation. This is evident from the fact that the doping of free dopamine molecules within the HA-CS gels was found to be deleterious and suppressed the differentiation of neuronal differentiation of stem cells. Thus, the HADA-CS matrix is a promising tool for tailoring brain mimetic scaffolds and neuronal tissue engineering applications.

Declaration of Competing Interest

The authors declare that they have no known competing financial interests or personal relationships that could have appeared to influence the work reported in this paper.

Acknowledgments

The work was supported by the Imaging Facility and iPS Cells Facility (Faculty of Medicine and Health Technology, Tampere University). The authors also thank Biocenter Finland for the support of Imaging and iPS cell facilities. This work was supported by the Academy of Finland (grant number 336665 to SN; grant numbers 286990, 326436, and 301824 to LY), the European Union's Horizon 2020 Marie Sklodowska-Curie Grant Program (Agreement No. 713645 to SS). We thank Prof. Vesa Hytönen, Faculty of Medicine and Health Technology, Tampere University, and Austin D. Evans, Tampere University for assisting with osmolality measurements of the hydrogels.

References

[1] K. Shi, D.C. Tian, Z.G. Li, A.F. Ducruet, M.T. Lawton, F.D. Shi, Global brain inflammation in stroke, Lancet Neurol. 18 (2019) 1058–1066, doi:10.1016/S1474-4422(19)30078-X.
[2] V. Dinet, K.G. Petry, J. Badaut, Brain–immune interactions and neuroinflammation after traumatic brain injury, Front. Neurosci. 13 (2019) 1178, doi:10.3389/fnins.2019.01178.
[3] J. Lam, W.E. Lowry, S.T. Carmichael, T. Segura, Delivery of iPS-NPCs to the stroke cavity within a hyaluronic acid matrix promotes the differentiation of transplanted cells, Adv. Funct. Mater. 24 (2014) 7053–7062, doi:10.1002/adfm.201401483.
[4] G.D. Mahumane, P. Kumar, L.C. Du Toit, Y.E. Choonara, V. Pillay, 3D scaffolds for brain tissue regeneration: architectural challenges, Biomater. Sci. 6 (2018) 2812–2837, doi:10.1039/c8bm00422f.
[5] V.D. Ranjan, L. Qiu, J.W.L. Lee, X. Chen, S.E. Jang, C. Chai, K.L. Lim, E.K. Tan, Y. Zhang, W.M. Huang, L. Zeng, A microfiber scaffold-based 3D: in vitro human neuronal culture model of Alzheimer's disease, Biomater. Sci. 8 (2020) 4861–4874, doi:10.1039/d0bm00833h.
[6] J. Kajtez, F. Nilsson, A. Fiorenzano, M. Parmar, J. Emnéus, 3D biomaterial models of human brain disease, Neurochem. Int. 147 (2021) 105043, doi:10.1016/j.neuint.2021.105043.
[7] S.A. Langhans, Three-dimensional in vitro cell culture models in drug discovery and drug repositioning, Front. Pharmacol. 9 (2018) 6, doi:10.3389/fphar.2018.00006.
[8] M. Piantino, A. Figarol, M. Matsusaki, Three-dimensional in vitro models of healthy and tumor brain microvasculature for drug and toxicity screening, Front. Toxicol. 3 (2021) 656254, doi:10.3389/ftox.2021.656254.
[9] J. Wang, R. Chu, N. Ni, G. Nan, The effect of Matrigel as scaffold material for neural stem cell transplantation for treating spinal cord injury, Sci. Rep. 10 (2020) 1–11, doi:10.1038/s41598-020-59148-3.
[10] A.M. Hopkins, L. De Laporte, F. Tortelli, E. Spedden, C. Staii, T.J. Atherton, J.A. Hubbell, D.L. Kaplan, Silk hydrogels as soft substrates for neural tissue engineering, Adv. Funct. Mater. 23 (2013) 5140–5149, doi:10.1002/adfm.201300435.
[11] Y.T.L. Dingle, V. Liaudanskaya, L.T. Finnegan, K.C. Berlind, C. Mizzoni, I. Georgakoudi, T.J.F. Nieland, D.L. Kaplan, Functional characterization of three-dimensional cortical cultures for in vitro modeling of brain networks, IScience 23 (2020) 101434, doi:10.1016/J.ISCI.2020.101434.
[12] A. Bozza, E.E. Coates, T. Incitti, K.M. Ferlin, A. Messina, E. Menna, Y. Bozzi, J.P. Fisher, S. Casarosa, Neural differentiation of pluripotent cells in 3D alginate-based cultures, Biomaterials 35 (2014) 4636–4645, doi:10.1016/j.biomaterials.2014.02.039.
[13] J. Kapr, L. Petersilie, T. Distler, I. Lauria, F. Bendt, C.M. Sauter, A.R. Boccaccini, C.R. Rose, E. Fritsche, Human induced pluripotent stem cell-derived neural progenitor cells produce distinct neural 3D in vitro models depending on alginate/gellan gum/laminin hydrogel blend properties, Adv. Healthc. Mater. (2021) 2100131, doi:10.1002/ADHM.202100131.
[14] O.M. Fannon, A. Bithell, B.J. Whalley, E. Delivopoulos, A fiber alginate co-culture platform for the differentiation of mESC and modeling of the neural tube, Front. Neurosci. (2020) 14, doi:10.3389/FNINS.2020.524346.
[15] Z. Wei, J. Zhao, Y.M. Chen, P. Zhang, Q. Zhang, Self-healing polysaccharide-based hydrogels as injectable carriers for neural stem cells, Sci. Rep. 6 (2016) 1–12, doi:10.1038/srep37841.
[16] W. Lee, C.W. Frank, J. Park, Directed axonal outgrowth using a propagating gradient of IGF-1, Adv. Mater. 26 (2014) 4936–4940, doi:10.1002/adma.201305995.
[17] J.A. Crowe, A. El-Tamer, D. Nagel, A.V. Koroleva, J. Madrid-Wolff, O.E. Olarte, S. Sokolovsky, E. Estevez-Priego, A.-A. Ludl, J. Soriano, P. Loza-Alvarez, B.N. Chichkov, E.J. Hill, H.R. Parri, E.U. Rafailov, Development of two-photon polymerised scaffolds for optical interrogation and neurite guidance of human iPSC-derived cortical neuronal networks, Lab Chip 20 (2020) 1792–1806, doi:10.1039/C9LC01209E.
[18] A. Koroleva, A. Deiwick, A. El-Tamer, L. Koch, Y. Shi, E. Estévez-Priego, A.-A. Ludl, J. Soriano, D. Guseva, E. Ponimaskin, B. Chichkov, In vitro development of human iPSC-derived functional neuronal networks on laser-fabricated 3D scaffolds, ACS Appl. Mater. Interfaces 13 (2021) 7839–7853, doi:10.1021/ACSAMI.0C16616.
[19] M. Bosiacki, M. Gąssowska-Dobrowolska, K. Kojder, M. Fabiańska, D. Jeżewski, I. Gutowska, A. Lubkowska, Perineuronal nets and their role in synaptic homeostasis, Int. J. Mol. Sci. 20 (2019), doi:10.3390/ijms20174108.
[20] N. Broguiere, L. Isenmann, M. Zenobi-Wong, Novel enzymatically cross-linked hyaluronan hydrogels support the formation of 3D neuronal networks, Biomaterials 99 (2016) 47–55, doi:10.1016/j.biomaterials.2016.04.036.
[21] L. Karumbaiah, S.F. Enam, A.C. Brown, T. Saxena, M.I. Betancur, T.H. Barker, R.V. Bellamkonda, Chondroitin sulfate glycosaminoglycan hydrogels create endogenous niches for neural stem cells, Bioconjug. Chem. 26 (2015) 2336–2349, doi:10.1021/acs.bioconjchem.5b00397.
[22] L. Ylä-Outinen, V. Harju, T. Joki, J.T. Koivisto, J. Karvinen, M. Kellomäki, S. Narkilahti, Screening of hydrogels for human pluripotent stem cell–derived neural cells: hyaluronan-polyvinyl alcohol-collagen-based interpenetrating polymer network provides an improved hydrogel scaffold, Macromol. Biosci. 19 (2019) 1900096, doi:10.1002/mabi.201900096.
[23] L. Honkamäki, T. Joki, N.A. Grigoryev, K. Levon, L. Ylä-Outinen, S. Narkilahti, Novel method to produce a layered 3D scaffold for human pluripotent stem cell-derived neuronal cells, J. Neurosci. Methods 350 (2021) 109043, doi:10.1016/j.jneumeth.2020.109043.
[24] A. Napoli, I. Obeid, Comparative analysis of human and rodent brain primary neuronal culture spontaneous activity using micro-electrode array technology, J. Cell. Biochem. 117 (2016) 559–565, doi:10.1002/jcb.25312.
[25] X. Zhao, A. Bhattacharyya, Human models are needed for studying human neurodevelopmental disorders, Am. J. Hum. Genet. 103 (2018) 829–857, doi:10.1016/j.ajhg.2018.10.009.
[26] C.M. Madl, B.L. LeSavage, R.E. Dewi, K.J. Lampe, S.C. Heilshorn, Matrix remodeling enhances the differentiation capacity of neural progenitor cells in 3D hydrogels, Adv. Sci. 6 (2019) 1801716, doi:10.1002/advs.201801716.
[27] H. Fujioka, Y. Dairyo, K.I. Yasunaga, K. Emoto, Neural Functions of Matrix Metalloproteinases: Plasticity, Neurogenesis, and Disease, Biochem. Res. Int, 2012, doi:10.1155/2012/789083.
[28] A. Hyysalo, M. Ristola, M.E.L. Mäkinen, S. Häyrynen, M. Nykter, S. Narkilahti, Laminin $\alpha 5$ substrates promote survival, network formation and functional development of human pluripotent stem cell-derived neurons in vitro, Stem Cell Res. 24 (2017) 118–127, doi:10.1016/j.scr.2017.09.002.
[29] R. Patel, M. Santhosh, J.K. Dash, R. Karpoormath, A. Jha, J. Kwak, M. Patel, J.H. Kim, Ile-Lys-Val-ala-Val (IKVAV) peptide for neuronal tissue engineering, Polym. Adv. Technol. 30 (2019) 4–12, doi:10.1002/pat.4442.
[30] P.B. Welzel, S. Prokoph, A. Zieris, M. Grimmer, S. Zschoche, U. Freudenberg, C. Werner, Modulating biofunctional starPEG heparin hydrogels by varying size and ratio of the constituents, Polymer 3 (2011) 602–620 2011, Vol. 3, Pages 602-620, doi:10.3390/POLYM3010602.
[31] T. Hyvärinen, A. Hyysalo, F.E. Kapucu, L. Aarnos, A. Vinogradov, S.J. Eglen, L. Ylä-Outinen, S. Narkilahti, Functional characterization of human pluripotent stem cell-derived cortical networks differentiated on laminin-521 substrate: comparison to rat cortical cultures, Sci. Rep. 9 (2019) 1–15, doi:10.1038/s41598-019-53647-8.
[32] J.T. Koivisto, T. Joki, J.E. Parraga, R. Paakkönen, L. Yla-Outinen, L. Salonen, I. Jönkkari, M. Peltola, T.O. Ihalainen, S. Narkilahti, M. Kellomaki, Bioamine-

crosslinked gellan gum hydrogel for neural tissue engineering, Biomed. Mater. 12 (2017) 025014, doi:10.1088/1748-605X/aa62b0.
[33] L. Djerbal, H. Lortat-Jacob, J. Kwok, Chondroitin sulfates and their binding molecules in the central nervous system, Glycoconj. J. 34 (2017) 363–376, doi:10.1007/s10719-017-9761-z.
[34] J. Iida, A.M.L. Meijne, T.R. Oegema, T.A. Yednock, N.L. Kovach, L.T. Furcht, J.B. McCarthy, A role of chondroitin sulfate glycosaminoglycan binding site in $\alpha 4\beta 1$ integrin-mediated melanoma cell adhesion, J. Biol. Chem. 273 (1998) 5955–5962, doi:10.1074/jbc.273.10.5955.
[35] M.I. Betancur, H.D. Mason, M. Alvarado-Velez, P.V. Holmes, R.V. Bellamkonda, L. Karumbaiah, Chondroitin sulfate glycosaminoglycan matrices promote neural stem cell maintenance and neuroprotection post-traumatic brain injury, ACS Biomater. Sci. Eng. 3 (2017) 420–430, doi:10.1021/acsbiomaterials.6b00805.
[36] O.P. Oommen, S. Wang, M. Kisiel, M. Sloff, J. Hilborn, O.P. Varghese, Smart design of stable extracellular matrix mimetic hydrogel: Synthesis, characterization, and in vitro and in vivo evaluation for tissue engineering, Adv. Funct. Mater. 23 (2013) 1273–1280, doi:10.1002/adfm.201201698.
[37] M. Kisiel, M. Ventura, O.P. Oommen, A. George, X.F. Walboomers, J. Hilborn, O.P. Varghese, Critical assessment of rhBMP-2 mediated bone induction: An in vitro and in vivo evaluation, J. Control. Rel. 162 (2012) 646–653, doi:10.1016/j.jconrel.2012.08.004.
[38] L. Koivusalo, M. Kauppila, S. Samanta, V.S. Parihar, T. Ilmarinen, S. Miettinen, O.P. Oommen, H. Skottman, Tissue adhesive hyaluronic acid hydrogels for sutureless stem cell delivery and regeneration of corneal epithelium and stroma, Biomaterials 225 (2019), doi:10.1016/j.biomaterials.2019.119516.
[39] R.E. Van Kesteren, G.E. Spencer, The role of neurotransmitters in neurite outgrowth and synapse formation, Rev. Neurosci. 14 (2003) 217–231, doi:10.1515/REVNEURO.2003.14.3.217.
[40] W. Hu, Z. Wang, Y. Xiao, S. Zhang, J. Wang, Advances in crosslinking strategies of biomedical hydrogels, Biomater. Sci. 7 (2019) 843–855, doi:10.1039/c8bm01246f.
[41] T.H. Perera, X. Lu, L.A. Smith Callahan, Effect of laminin derived peptides IKVAV and LRE tethered to hyaluronic acid on hiPSC derived neural stem cell morphology, attachment and neurite extension, J. Funct. Biomater. 11 (2020) 15, doi:10.3390/jfb11010015.
[42] D. Bermejo-Velasco, G.N. Nawale, O.P. Oommen, J. Hilborn, O.P. Varghese, Thiazolidine chemistry revisited: a fast, efficient and stable click-type reaction at physiological pH, Chem. Commun. 54 (2018) 12507–12510, doi:10.1039/c8cc05405c.
[43] J. Gao, Y.M. Kim, H. Coe, B. Zern, B. Sheppard, Y. Wang, A neuroinductive biomaterial based on dopamine, Proc. Natl. Acad. Sci. USA 103 (2006) 16681–16686, doi:10.1073/pnas.0606237103.
[44] X. Zhou, H. Cui, M. Nowicki, S. Miao, S.J. Lee, F. Masood, B.T. Harris, L.G. Zhang, Three-dimensional-bioprinted dopamine-based matrix for promoting neural regeneration, ACS Appl. Mater. Interfaces 10 (2018) 8993–9001, doi:10.1021/acsami.7b18197.
[45] E. Cuadrado, A. Rosell, A. Penalba, M. Slevin, J. Alvarez-Sabín, A. Ortega-Aznar, J. Montaner, Vascular MMP-9/TIMP-2 and neuronal MMP-10 up-regulation in human brain after stroke: a combined laser microdissection and protein array study, J. Proteome Res. 8 (2009) 3191–3197, doi:10.1021/pr801012x.
[46] C. Daly, E.B. Ziff, Post-transcriptional regulation of synaptic vesicle protein expression and the developmental control of synaptic vesicle formation, J. Neurosci. 17 (1997) 2365–2375, doi:10.1523/JNEUROSCI.17-07-02365.1997.
[47] E. Moutaux, W. Christaller, C. Scaramuzzino, A. Genoux, B. Charlot, M. Cazorla, F. Saudou, Neuronal network maturation differently affects secretory vesicles and mitochondria transport in axons, Sci. Rep. 81 (8) (2018) 1–14 2018, doi:10.1038/s41598-018-31759-x.